Ab initio modeling of dynamic stability of silicon prismanes

M. A. Gimaldinova[1,2], A. I. Kochaev[3], M. M. Maslov[†,1,2]

†Mike.Maslov@gmail.com

[1]National Research Nuclear University MEPhI, 31 Kashirskoe shosse, Moscow, 115409, Russia
[2]Research Institute for the Development of Scientific and Educational Potential of Youth,
14/55 Aviatorov St., Moscow, 119620, Russia
[3]Ulyanovsk State University, 42 Leo Tolstoy St., Ulyanovsk, 432017, Russia

We present the results of a study on the dynamic stability of silabiprismanes by means of the density functional theory. Silabiprismanes present an elementary case of a particular type of silicon nanotubes with an extremely small cross-section, constructed from dehydrogenated molecules of cyclosilanes (silicon rings). Unlike higher polysilaprismanes, they are formed by only three silicon rings and described by the chemical formula $(Si_n)_3H_{2n}$. In the presented study, we limited ourselves to the cases $n = 5 \div 7$. We focused on a detailed review of the mechanisms of isomerization and decomposition. Configurations of the corresponding transition states were determined, and the kinetic parameters in the Arrhenius law (activation energy and frequency factor) were evaluated. Silabiprismanes are found to be much more stable compounds than their carbon analogous. Their lifetimes at room temperature achieve hundreds of seconds, but at 200 K, their stability increases significantly. Thus, their lifetimes are sufficiently high for the identifying and studying of silicon biprismanes, but not for their industrial applications. Therefore, unsubstituted silabiprismanes require lower temperatures of operation, and their applicability is restricted. Although the general pyrolysis path is the same for all considered cages, its features strongly and non-monotonically depend on n. It is confirmed that the hexagonal and heptagonal silabiprismanes are much more stable than the pentagonal one. We obtained the absence of a direct correlation between the thermodynamic and kinetic stabilities of the silicon cages under consideration.

Keywords: silaprismanes, transition state, activation energy, cage breaking, density functional theory.

Квантово-химическое моделирование динамической устойчивости кремниевых призманов

Гимальдинова М. А.[1,2], Кочаев А. И.[3], Маслов М. М.[†,1,2]

[1]Национальный исследовательский ядерный университет «МИФИ», Каширское ш., 31, Москва, 115409, Россия
[2]Научно-исследовательский институт проблем развития научно-образовательного потенциала молодёжи,
ул. Авиаторов, 14/55, Москва, 119620, Россия
[3]Ульяновский государственный университет, ул. Л. Толстого, 42, Ульяновск, 432017, Россия

Представлены результаты анализа динамической устойчивости силабипризманов, полученные с помощью теории функционала плотности. Силабипризманы являются элементарными представителями особого класса кремниевых нанотрубок с экстремально малым поперечным сечением, построенных из дегидрированных молекул циклосиланов (кремниевых колец). В отличие от высших полисилапризманов, они образованы лишь тремя кремниевыми кольцами и описываются химической формулой $(Si_n)_3H_{2n}$. В представленном исследовании мы ограничились случаями с $n = 5 \div 7$. В работе представлен подробный анализ механизмов их изомеризации и разложения. Нами определены атомные конфигурации соответствующих переходных состояний и оценены термокинетические параметры в законе Аррениуса (энергия активации и частотный фактор). Установлено, что силабипризманы являются гораздо более устойчивыми соединениями, чем их углеродные аналоги. Времена их жизни при комнатной температуре (300 K) достигают нескольких сотен секунд, при 200 K их стабильность существенно увеличивается. Таким образом, их времена жизни достаточно высоки для экспериментальной идентификации и дальнейших лабораторных исследований, однако могут оказаться недостаточными для их промышленного применения. Следовательно,

незамещенные силабипризманы требуют более низких температур эксплуатации, и их широкое применение ограничено. Хотя общий механизм пиролиза одинаков для всех рассматриваемых наноструктур, его особенности существенно и немонотонно зависят от *n*. Нами дополнительно подтверждено, что силабипризманы, построенные из шести- и семичленных кремниевых колец, гораздо более устойчивы, чем те, которые построены из пентагонов. При этом, прямая корреляция между термодинамической и кинетической устойчивостью рассматриваемых кремниевых каркасов отсутствует.

Ключевые слова: силапризманы, переходное состояние, энергия активации, разрушение каркаса, теория функционала плотности.

1. Introduction

For traditional carbon materials, the typical value of the valence angles between two covalent bonds is close to 120° (sp^2 hybridization) or 109.5° (sp^3 hybridization). A significant deviation of the valence angles from these values usually results in high strains and low stability of the system. However, some novel carbon architectures (fullerites [1], curved nanotubes [2], 4–8 graphene sheets [3], diamond-like phases, based on nanotubes [4] or graphene [5], hypercubane [6], etc.) include the valence angles of 90°.

Carbon polyprismanes are the most common class of materials in which C-C bonds are perpendicular to each other [7]. They are constructed from two or more flat regular polygons, which form a prismatic cage. Prism vertices are passivated by hydrogens to saturate the fourth valence of carbon atoms. The simplest prismane, hydrocarbon cubane C_8H_8 with a cubic carbon skeleton, was first synthesized by Eaton and Cole in 1964 [8]. It can be functionalized by different chemical groups and forms several stable derivatives. Later, other carbon prismanes consisted of two conjugated triangles [9] or pentagons [10] were prepared. The feasibility of more extended prismatic structures consisted of many attached polygons was predicted by extensive *ab initio* calculations [11,12]. According to Ref. [12], the thermodynamic stability of prismanes monotonically increases with their lengths.

Silicon analogs of carbon prismanes (silaprismanes) have been also intensively studied. They are more stable than their carbon counterparts [13]. To date, only some simplest silaprismanes have been synthesized [14,15]. However, the structure and properties of higher silaprismanes were theoretically predicted [16]. It is very surprising that the rather long "infinite" silaprismanes possess metallic conductivity, despite their sp^3 hybridization [17]. Binding energies of silaprismanes increases with their lengths [16]. A particular type of aromaticity ("cylindrical aromaticity") contributes to their stability [18,19]. Earlier endohedral silaprismane Si@$Si_{18}H_{12}$ was assumed to be the lowest energy Si-H structure [20], because it can be obtained as a result of self-assembly of small Si-H molecules. However, more feasible Si-H clusters were found later [21,22]. Therefore, prismanes and their derivatives are not low-energy isomers of Si-H systems. Since prismanes are metastable structures, their cages break at high temperatures. The breaking rate is defined by the corresponding activation barrier, which can be considered as a suitable measure of the kinetic stability of the system. The stability of silaprismanes plays a crucial role in their practical applications, especially at high temperatures. In this Letter, we consider silicon biprismanes — the simplest three-layered prismanes, which are intermediate systems

between classical prismanes and elongated 1D polyprismanes. We calculate activation barriers for $(Si_n)_3H_{2n}$ ($n = 5 \div 7$) systems and evaluate their kinetic stability. We chose the *n* values to be close to six, because this provides feasible values of valence angles in polygonal rings of prismane (close to 120°).

2. Materials and methods

Atomic structures of the considered three-layered silaprismanes $(Si_n)_3H_{2n}$ ($n = 5 \div 7$) are presented in Fig. 1. We are interested in the activation barrier for the breaking of their frames at high temperatures. Earlier, the channel of pyrolysis of the $Si_{18}H_{12}$ silaprismane was revealed via molecular dynamic simulations [23]. According to the mentioned study [23], cage destabilization starts from the breaking of the Si-Si bond in the middle hexagonal ring. We adobe the same mechanism for the other studied silaprismanes. To find the reaction minimal energy path, we gradually increase the length of the breaking bond by steps of 0.002 Å and freeze it, whereas all other internal coordinates were optimized using the standard BFGS algorithm. The configuration with the highest energy is regarded as the first approximation to the transition state, corresponding to the top of the energy barrier. This configuration is further optimized to locate the transition state more accurately. The Hessian calculation confirms that the obtained configuration has only one imaginary frequency. The described approach is suitable for simple reactions and possesses much better performance and convergence than the common nudged elastic bands algorithm. It should be preferably applied when the reaction mechanism is preliminary known [24]. Energy barrier *U* is estimated as the energy difference between the ground and transition configurations. Frequency factor *A* is derived from the eigenfrequencies of the ground and transition states according to the Vineyard formula [25]:

$$A = \frac{\prod_{i=1}^{3N-6} w_i}{\prod_{i=1}^{3N-7} w'_i},$$

where $N = 5n$ is the total number of atoms in biprismane, $3N-6$, and $3N-7$ are the whole numbers of real eigenfrequencies w and w' that correspond to the ground and transition states, respectively.

All quantum chemical simulations were performed using the density functional theory approach realized in GAMESS software [26]. Standard B3LYP hybrid functional [27,28] with 6-31G(d) electronic basis set [29] were used in all calculations. We keep unchanged all default numerical thresholds adopted in GAMESS.
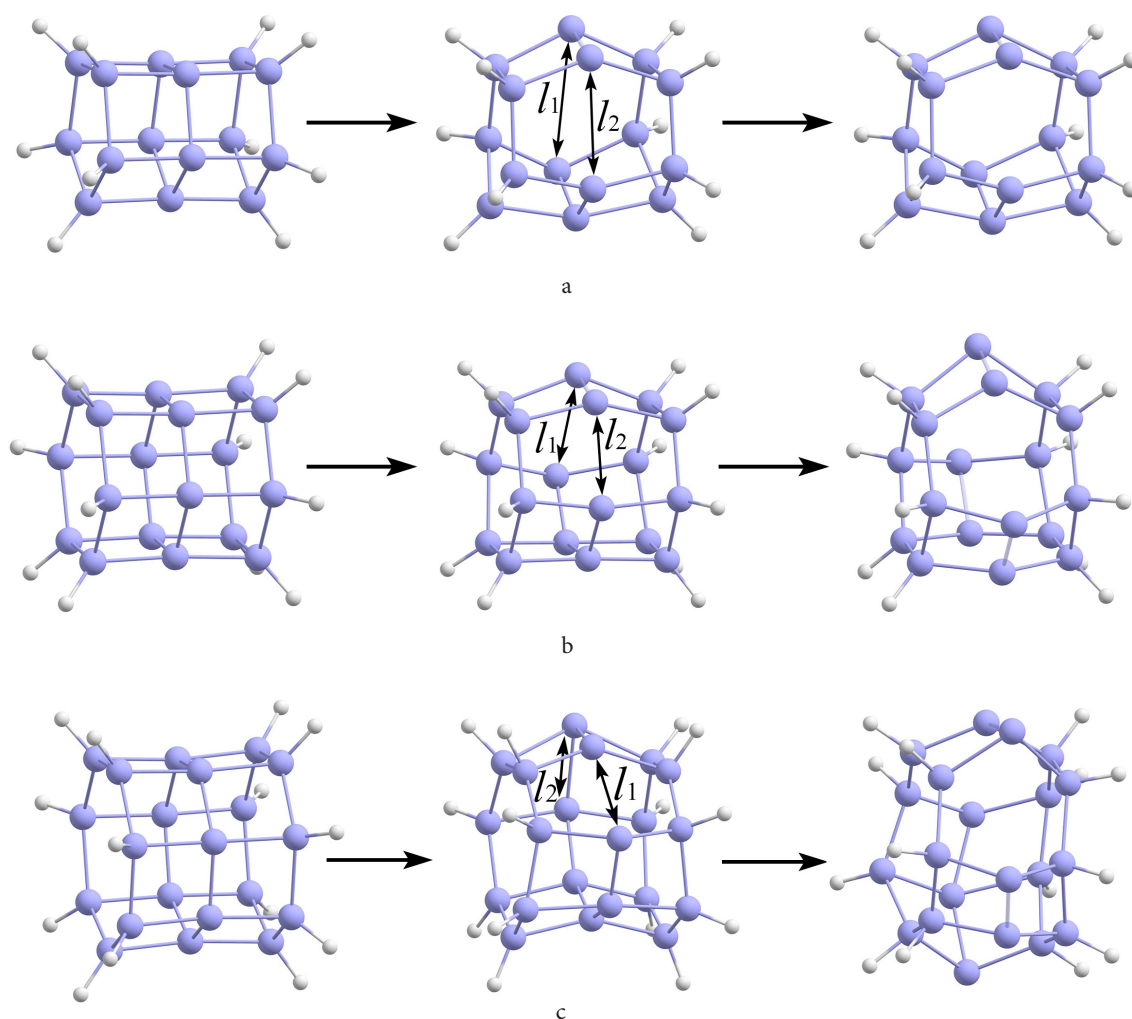
Fig. 1. (Color online) Atomic structures of initial, transition, and final configurations of silicon biprismanes $(Si_5)_3H_{10}$ (a), $(Si_6)_3H_{12}$ (b), and $(Si_7)_3H_{14}$ (c) during the decomposition. Lilac and white balls depict silicon and hydrogen atoms, respectively.

3. Results and discussions

Schematic paths of silicon cage breaking are presented in Fig. 1. At the initial stage, one of the Si-Si bonds in the middle polygonal ring (labeled as l_1) breaks. Simultaneously, another bond at the same ring (labeled as l_2) significantly elongates. The values of l_1 and l_2 corresponding to the configurations of the transition state are presented in Table 1. One can see the irregular and non-monotonic character of their dependence on n. This fact confirms that the reaction path is determined by the diameter of biprismane. Finally, the other bonds in the middle ring break and biprismane transforms into a spherical fullerene-like cluster, which can contain square, pentagon, hexagon, or heptagon rings on its surface (see Fig. 1). Note that all bonds that do not belong to the middle ring remain unbroken.

The values of U and A are also presented in Table 1. Barriers U are ~1 eV for both $Si_{18}H_{12}$ and $Si_{21}H_{14}$ biprismanes, and somewhat lower for $Si_{15}H_{10}$ cage. All obtained barriers are much higher than the corresponding values for similar carbon systems. For example, previously reported barriers for carbon pentagonal biprismane $C_{15}H_{10}$ and hexagonal prismane $C_{12}H_{12}$ are equal to 0.41 [30] and 0.59 eV [31], respectively. Calculated barriers for silaprismanes are close

to the barrier for cyclotetracubyl $(C_8H_6)_4$ (1.1 eV [32]), which is known as a relatively stable compound. So, silicon biprismanes are quite kinetically stable. Frequency factors, calculated from the Vineyard formula, are typical for middle-sized atomic clusters. Typical lifetimes t of biprismanes at given temperature T can be evaluated using the kinetic parameters U and A from the Arrhenius law

$$t = \frac{1}{Ag} \exp\left(-\frac{U}{kT}\right),$$

where k is the Boltzmann's constant, g is the degeneration factor, corresponding to the number of equivalent reaction paths with the same activation barrier U. In our case, there are n equivalent Si-Si bonds l_1 in the middle biprismane ring. Moreover, there are two equivalent bonds l_2 for each chosen l_1. Therefore, we adopt $g = 2n$. Calculated values of t at cryogenic ($T = 200$ K) and room ($T = 300$ K) temperatures are also presented in Table 1. One can see that all considered systems are sufficiently stable to be synthesized and detected even at room temperatures. At lower temperatures ($T = 200$ K), their lifetimes are long enough for any application, whereas at the temperature of liquid nitrogen (77 K), lifetimes are practically infinite.

Table 1. Binding energies E_b of silicon prismanes. Lengths of breaking bonds l_1 and l_2 and imaginary frequencies of transition state configurations corresponding to the decomposition of silabiprismanes $(Si_{n'})_3 H_{2n'}$. Minimal energy barriers U and frequency factors A for cage breaking are also presented. Kinetic parameters U and A for the $Si_{18}H_{12}$ system coincide with the previously reported values extracted from molecular dynamics calculations [23]. Average lifetimes t calculated from the Arrhenius law are given for cryogenic (77 K), low (200 K), and room (300 K) temperatures.

Prismane	n	E_b, eV/atom	l_1, Å	l_2, Å	w, cm^{-1}	U, eV	A, s^{-1}	t, s (77 K)	t, s (200 K)	t, s (300 K)
$Si_{15}H_{10}$	5	4.67	4.535	3.638	$36i$	0.77	$4.1{\cdot}10^{13}$	$5.9{\cdot}10^{35}$	$6.1{\cdot}10^{4}$	$2.1{\cdot}10^{-2}$
$Si_{18}H_{12}$	6	4.67	3.996	3.136	$166i$	1.09	$6.6{\cdot}10^{14}$	$2.3{\cdot}10^{55}$	$3.7{\cdot}10^{11}$	$2.6{\cdot}10^{2}$
$Si_{21}H_{14}$	7	4.62	4.347	2.705	$43i$	1.03	$5.4{\cdot}10^{13}$	$3.3{\cdot}10^{52}$	$1.2{\cdot}10^{11}$	$2.6{\cdot}10^{2}$

There is no direct relationship between the thermodynamic stability determined by the binding energy, and the kinetic stability determined by the energy barrier. For example, pentagonal and hexagonal biprismanes possess approximately the same thermodynamic stability [16], whereas their kinetic stabilities are quite different. We calculated the binding energies of the considered silicon prismanes as a measure of their thermodynamic stability according to the formula $E_b = \left(3nE\left(\text{Si}\right) + 2nE\left(\text{H}\right) - E\left(\text{Si}_{3n}\text{H}_{2n}\right)\right)/5n$ at the same level of theory B3LYP/6-31G(d). The values of these binding energies are presented in Table 1. Therefore, the dynamic stability of highly strained molecules should be studied regardless of their binding energies.

4. Conclusions

At present, we can see a great advantage of novel carbon nanostructures over traditional materials. They possess a wide range of physical and chemical properties useful for nanoelectronics and other applications. Silicon nanostructures are still less studied. However, already existing technological equipment in the field of electronics deals with silicon materials. Therefore, novel silicon forms have more chances to be widely applied in industry. Most carbon architectures have their silicon analogous, which are potentially useful and interesting to study.

In the presented Letter, we analyze the thermal stability of silicon biprismanes, which are the first step from classical prismanes toward to quasi-one-dimensional polyprismane wires. Interest in polyprismanes is associated with their unique electronic properties. They combine sp^3 hybridization, leading to low reactivity with the high metallic-like conductivity. The thermal stability of these systems plays a crucial role in the suitability of their use in practical applications.

Our calculations confirm the moderate stability of silicon biprismanes at room temperatures. Their lifetimes are sufficiently high for the identifying and studying of biprismanes, but not for their industrial applications. So, unsubstituted biprismanes require lower temperatures of operation, and their applicability is restricted. However, there are several ways to improve their stability, for example, substitutional doping or the creation of molecular crystals based on them similar to fullerites.

References

1. L. K. Rysaeva, J. A. Baimova, D. S. Lisovenko, V. A. Gorodtsov, S. V. Dmitriev. Phys. Status Solidi B. 2018, 1800049 (2018). Crossref
2. E. A. Belenkov, Y. A. Zinatulina. Phys. Solid State. 52 (4), 868 (2010). Crossref
3. E. A. Belenkov, V. V. Mavrinskii, V. A. Greshnyakov, M. M. Brzhezinskaya. IOP Conf. Series: Materials Science and Engineering. 537, 022070 (2019). Crossref
4. L. K. Rysaeva, J. A. Baimova, S. V. Dmitriev, D. S. Lisovenko, V. A. Gorodtsov, A. I. Rudskoy. Diamond and Related Materials. 97, 107411 (2019). Crossref
5. L. K. Rysaeva, D. S. Lisovenko, V. A. Gorodtsov, J. A. Baimova. Comp. Mat. Sci. 172, 109355 (2019). Crossref
6. F. Pichierri. Chem. Phys. Lett. 612, 198 (2014). Crossref
7. E. G. Lewars. Modeling Marvels: Computational Anticipation of Novel Molecules. The Netherlands, Dordrecht, Springer (2008) 282p. Crossref
8. P. E. Eaton, T. W. Cole Jr. J. Am. Chem. Soc. 86, 3157 (1964). Crossref
9. T. J. Katz, N. Acton. J. Am. Chem. Soc. 95 (8), 2738 (1973). Crossref
10. P. E. Eaton, Y. S. Or, S. J. Branca. J. Am. Chem. Soc. 103 (8), 2134 (1981). Crossref
11. S. Kuzmin, W. W. Duley. Fullerenes, Nanotubes and Carbon Nanostructures. 20 (8), 730 (2012). Crossref
12. K. P. Katin, S. A. Shostachenko, A. I. Avkhadieva, M. M. Maslov. Advances in Physical Chemistry. 2015, 506894 (2015). Crossref
13. A. Equbal, S. Srinivasan, N. Sathyamurthy. J. Chem. Sciences. 129 (7), 911 (2017). Crossref
14. H. Matsumoto, K. Higuchi, S. Kyushin, M. Goto. Angewandte Chemie International Edition in English. 31 (10), 1354 (1992). Crossref
15. A. Sekiguchi, T. Yatabe, C. Kabuto, H. Sakurai. J. Am. Chem. Soc. 115 (13), 5853 (1993). Crossref
16. M. A. Gimaldinova, K. P. Katin, M. A. Salem, M. M. Maslov. Lett. Mater. 8 (4), 454 (2018). Crossref
17. K. P. Katin, K. S. Grishakov, M. A. Gimaldinova, M. M. Maslov. Comp. Mat. Sci. 174, 109480 (2020). Crossref
18. H. Vach. Chem. Phys. Lett. 614 (2014), 199 (2014). Crossref
19. L. V. Duong, E. Matito, M. Solà, H. Behzadi, M. T. Nguyen, M. J. Momeni. Phys. Chem. Chem. Phys. 20, 23467 (2018). Crossref
20. H. Vach. Nano Letters. 11 (12), 5477 (2011). Crossref

21. G. A. Dolgonos, K. Mekalka. J. Comp. Chem. 36 (28), 2095 (2015). [Crossref](#)
22. M. V. Gordeychuk, K. P. Katin, K. S. Grishakov, M. M. Maslov. Int. J. Quantum Chemistry. 118 (15), e25609 (2018). [Crossref](#)
23. K. P. Katin, M. B. Javan, M. M. Maslov, A. Soltani. Chem. Phys. 487 (2017), 59 (2017). [Crossref](#)
24. D. W. Boukhvalov. Phys. Chem. Chem. Phys. 12 (47), 15367 (2010). [Crossref](#)
25. G. H. Vineyard. J. Phys. Chem. Sol. 3 (1-2), 121 (1957). [Crossref](#)
26. M. W. Schmidt, K. K. Baldridge, J. A. Boatz, S. T. Elbert, M. S. Gordon, J. H. Jensen, S. Koseki, N. Matsunaga, K. A. Nguyen, S. Su, T. L. Windus, M. Dupuis, J. A. Montgomery. J. Comp. Chem. 14 (11), 1347 (1993). [Crossref](#)
27. A. D. Becke. J. Chem. Phys. 98 (7), 5648 (1993). [Crossref](#)
28. C. Lee, W. Yang, R. G. Parr. Phys. Rev. B. 37 (2), 785 (1988). [Crossref](#)
29. R. Krishnan, J. S. Binkley, R. Seeger, J. A. Pople. J. Chem. Phys. 72 (1), 650 (1980). [Crossref](#)
30. K. P. Katin, M. M. Maslov. Molecular Simulation. 44 (9), 703 (2018). [Crossref](#)
31. S. A. Shostachenko, M. M. Maslov, V. S. Prudkovskii, K. P. Katin. Physics of the Solid State. 57 (5), 1023 (2015). [Crossref](#)
32. M. M. Maslov, K. P. Katin, A. I. Avkhadieva, A. I. Podlivaev. Russ. J. Phys. Chem. B. 8 (2), 152 (2014). [Crossref](#)